Investigation & Optimization of WEDM Process Parameters using Inconel 690

Sivanagaraju Dusanapudi[1*], *R L* Krupakaran[2], *Anshuman* Kumar[1], *K* Sai Venkat[1], Akash[1], Shanmukh[1], *Lalisetti* Ganesh[3], *Muntadar* Muhsen[4]

[1]Mechanical Engineering, Gokaraju Rangaraju Institute of Engineering and Technology, Hyderabad, Telangana, India.
[2]Department of Mechanical Engineering Mohan Babu University, Tirupati, Andhra Pradesh, India
[3]KG Reddy College of Engineering & Technology, Hyderabad, Telangana, India.
[4]Department of Refrigeration and air Conditioning Techniques engineering, College of technical engineering, The Islamic University, Najaf, Iraq.

Abstract. Wire Electrical Discharge Machining (WEDM) represents a pivotal process in the fabrication of high-strength materials such as Ni-based alloys, which find extensive application in aerospace and nuclear industries. In this study, the machining parameters have been considered as Spark on time (T_{on}), wire-speed (WS), Servo Sensitivity (FR), and gap voltage (GV). The machining performance on Inconel 690 has been identified with the help of Cutting speed (CS) and average Surface roughness (SR) through WEDM using Molybdenum (Mo) wire. Taguchi's philosophy has been considered in designing the experiments. The performance characteristics were analysed using a main effect plot and Analysis of Variance (ANOVA). The most significant parameter has been observed as T_{on}. Furthermore, a hybrid optimization technique has been employed using ANN coupled with MOJAYA to obtain the optimum machining parameters. The confirmation tests have been conducted has maximum percentage of error has been found as 7.88%. The said hybrid techniques was provided optimisation results within 4.65 seconds and identified as suitable techniques for optimisation results for Inconel-690

Keywords: ANN; Cutting speed; Inconel-690; MOJAYA; WEDM.

1 Introduction

The recent advancements in aircraft propulsion systems require a material with specific characteristics: thermal conductivity, wear resistance, and low chemical reactivity at high temperatures.[1]. Inconel alloys, renowned for their high performance, exhibit numerous essential characteristics ideal for diverse engineering applications, including the retention of acceptable strength at elevated temperatures. Among the Inconel alloy family, Inconel-690 (In-690) stands out for its compatibility with jet fuels in comparison to other grades of Inconel, alongside its exceptional weldability. Furthermore, In-690 finds widespread

* Corresponding Author: sivanagaraju.griet@gmail.com

application in turbine blades, nozzles, and other crucial hot-section components within jet engines.[2]. The use of In-690 in aircraft systems requires the formation of complex profiles.[3] In-690, despite its compatibility with traditional machining methods like milling and turning, exhibits heightened tool wear and internal stress formation during machining due to its high hardness. Conversely, non-traditional machining techniques, including WEDM, offer superior surface quality and tighter tolerances, particularly for intricate shapes.[4].Creating high-precision, top-quality products from this challenging-to-machine material poses a significant obstacle. Therefore, the manufacturing industry must adopt an effective and sustainable approach to balancing quality and productivity.[5]

Numerous research studies have explored the effects of WEDM process parameters on its performance. Ehsan Sagar et al. [6] found that increasing servo voltage enhanced surface finish. However, ANOVA analysis indicated minimal effects of Wire Tension and Wire speed on outcomes such as MRR and SR. Ramakrishnan et al. [7] identified ignition current, pulse on time, and delay time as the most influential parameters for machining Inconel 718 in WEDM. Tatjana V et al. [8] analyzed T_{on}, T_{off}, gap voltage, and wire feed, finding them significant factors affecting surface roughness and cutting speed. Y.S. Tarng et al. [9] developed a quadratic mathematical model using RSM, highlighting spark-on time as the most impactful parameter. Anshuman Kumar et al. [5] investigated spark-on time, flushing pressure, discharge current, and wire tension, concluding that Zn–WE exhibited higher MRR and lower SR. Yusliza Yusoff et al. [10] proposed an Ortho ANN model to predict machining performance on Inconel 718, reducing experimental trials by 99.2%. Pragya Shandilya et al. [11] suggested ANN-based optimization algorithms to determine optimal parameters for maximizing the cutting rate and minimizing surface roughness in WEDM of Inconel 825.

2 Experimental Procedures

In this investigation, we cut a plate of Inconel 690 measuring 300 x 200 x 5mm into specific sample pieces. Fig.2 illustrates the chemical composition of the work material under investigation. We used Molybdenum (Mo) wire to machine 18 specimens for the study, chosen based on prior research findings[12].

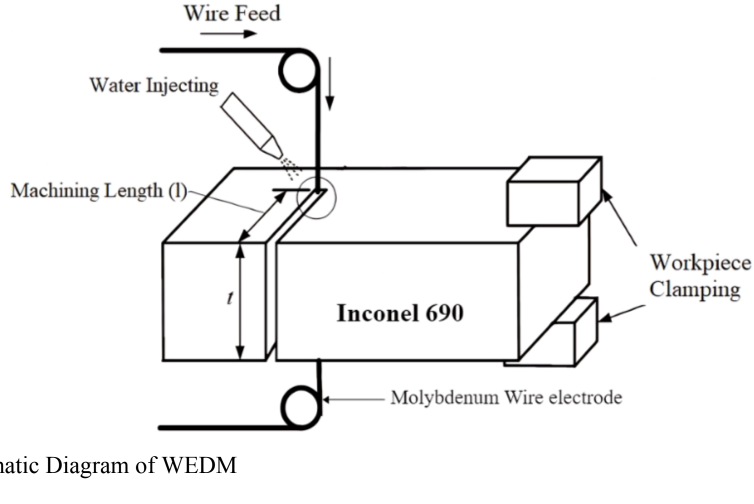

Fig.1. Schematic Diagram of WEDM

2.1 Material selection

We have selected Inconel-690 as the work material and outlined the results in Fig.2.

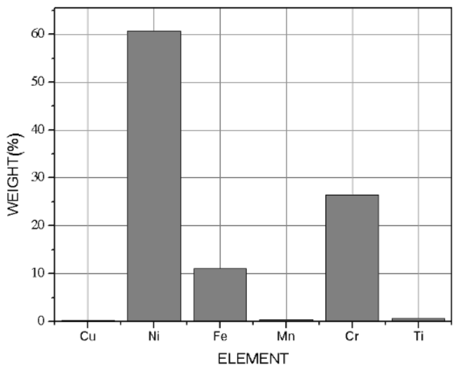

Fig. 2. Elemental composition of the received workpiece

2.2 Wire Electrode

In this experiment, we opted for a Molybdenum (Mo) wire with a diameter of 0.18mm as the tool electrode due to its high electrical and thermal conductivity, as well as its robustness, rigidity, and corrosion resistance.

Table 1. Properties of Mo Wire Electrode

Molecular Weight	95.94
Thermal Conductivity	1.38 W/cm/K at 298.2 K
Thermal Expansion	(25 °C) 4.8 $\mu m \cdot m^{-1} \cdot K^{-1}$
Vickers Hardness	1530 MPa
Young's Modulus	329 GPa

We employed Taguchi's L18 mixed OA for the experiment, incorporating four parameters: Spark on Time (T_{on}), Wire-Speed (WS), Servo Sensitivity (FR), and Gap Voltage (GV). We based the selection of these parameters on a literature review and the feasibility of the machine. We evaluated machining performance in this study based on surface roughness and cutting speed. We conducted the experiments using the Ezeecut NXG 3240, a CNC wire-cut EDM machine, with the experimental setup depicted in Fig.3(a). We used deionized water as the dielectric fluid throughout the experiment. Table 2 presents the details of the parameters and their levels. We recorded cutting speed values at the five corner points of the design and calculated their mean value for final consideration.

We removed the undesired foreign material particles from the WEDMed surface before taking SR measurements with the surface texture meter (Mitutoyo, product SJ-310, manufactured in Japan) to measure Surface Roughness (SR) {see Fig.3(b)}. We took SR measurements at five random locations on the WEDMed surface and used the averages of the SR values from five locations for analysis.

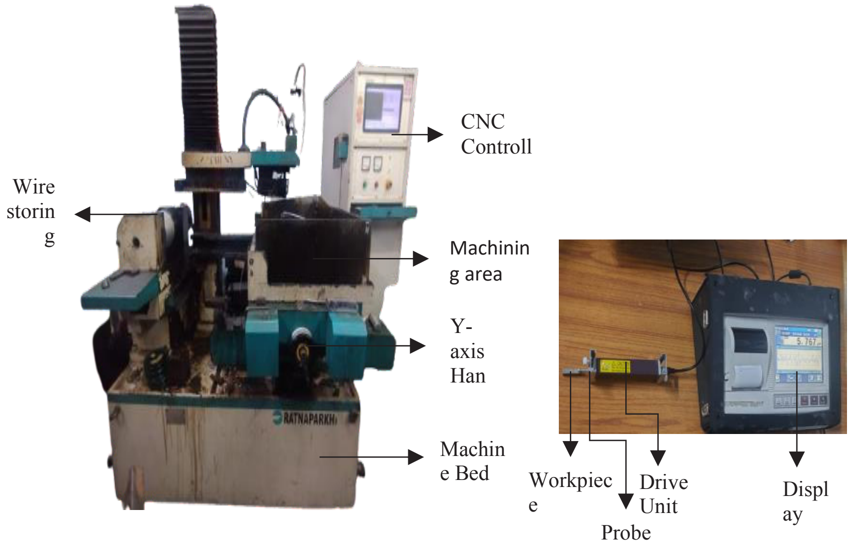

Fig.3. (a) Experimental Setup (**b)** Surface Roughness Setup

2.2 Input Process Parameters

Table 2. Parameter and its level

Code	Parameters	Unit	Levels		
			1	**2**	**3**
A	Spark on time (T_{on})	µs	32	36	-
B	Wire speed (WS)	mm/min	85	90	95
C	Servo Sensitivity (FR)	-	4	6	8
D	Gap Voltage (GV)	V	50	70	90
Fixed parameters					
Flushing pressure		bar	20		
Spark off time (T_{off})		µs	5		

3 Methodology

3.1 Artificial Neural Network (ANN)

Identifying an optimal combination of parameters in the manufacturing sector to simultaneously meet conflicting performance criteria, such as desiring higher cutting speed while minimizing surface roughness, poses a significant challenge. This challenge primarily arises from the complex mathematical calculations involved in the process and the significant computational time required. Artificial Neural Networks excel in managing non-linear relationships among input parameters to construct models and effectively handle multivariate data. They can process complex datasets and establish relationships between input and output variables, rendering them highly flexible and widely applicable in various research papers. Furthermore, ANN is highly flexible in modelling methods.

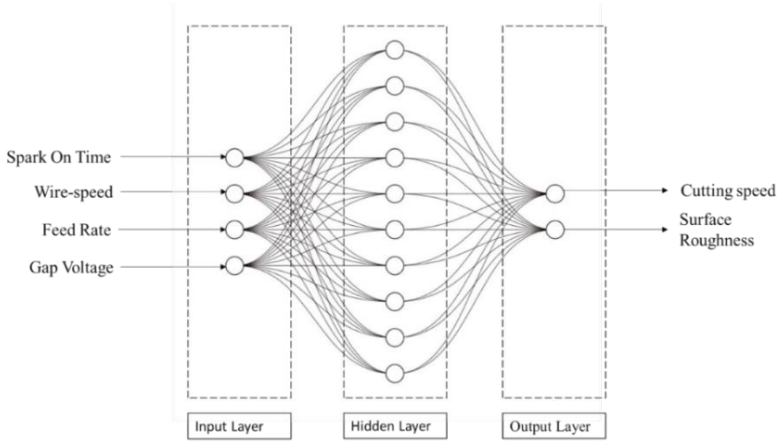

Fig. 4. Architecture of Artificial Neural Network

3.2 Mathematical model

We employed multivariable regression analysis to establish the relationship between input and responses. To address the complexity of this task, we need to generate nonlinear (multiplicative) models. We present the model in the following eq.(i).

$$y_1 = x_1 \times A^a \times B^b \times C^c \times D^d \qquad (i)$$

where, the variables A, B, C and D stand for T_{on}, WS, FR and GV. The nonlinear regression model utilized in this study was determined using the statistical software package MINITAB 21.

3.3 JAYA

The Jaya algorithm, which draws inspiration from natural selection and genetic evolution mechanisms, has been utilized in diverse domains such as engineering design, machine learning, and operations research.

The MOJAYA algorithm, an extended version of the JAYA algorithm tailored for multi-objective optimization, starts with a population of n particles. Each particle represents an m-dimensional vector, where m denotes the number of variables used in the optimization process. The computational process of MOJAYA emphasizes the following steps:

1. Randomly generate a population (X) of n individuals with m variables.
2. Calculate the objective function values for each individual in the population.
3. Perform non-dominated sorting on the population.
4. Compute the sharing fitness using Euclidean distance and niche count.
5. Update the population using eq.(ii).

$$X(t+1) = X(t) + r_1 \cdot (X_{best}(t) - |X(t)|) - r_2 \cdot (X_{worst}(t) - |X(t)|) \qquad (ii)$$

6. Reapply non-dominated sorting and compare with previous solutions, updating the population based on sharing fitness.
7. Repeat the algorithm through Steps 4 and 6 for 100 iterations to reach the Pareto optimal set.

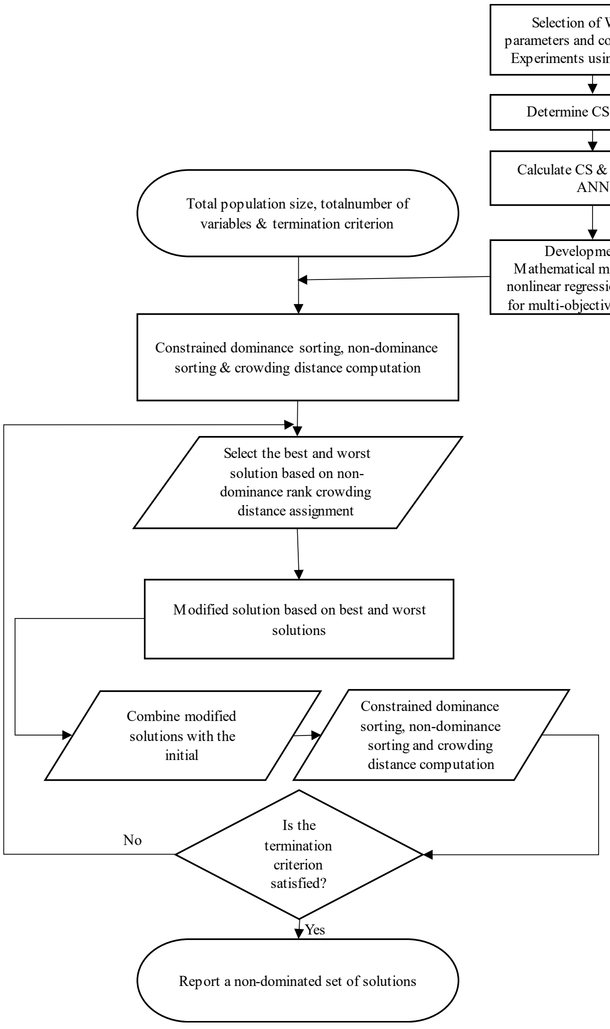

Fig. 5. Framework of the experimental study and proposed optimization route

4 Results and discussion

Table 3. Experimental data

S.no	T_{ON} (µs)	WS (mm/min)	FR	GV (V)	CS (mm/min)	SR (µm)	ANN CS	ANN SR
1	32	85	4	50	3.601	4.306	3.601	4.306
2	32	85	6	70	4.012	5.767	4.012	5.767
3	32	85	8	90	4.37	5.692	4.370	5.692
4	32	90	4	50	4.309	4.908	4.366	4.908
5	32	90	6	70	4.245	6.003	4.353	6.002
6	32	90	8	90	4.233	4.997	4.233	3.340
7	32	95	4	70	3.998	5.777	3.899	5.777

8	32	95	6	90	3.767	5.783	3.767	5.783
9	32	95	8	50	3.702	4.561	3.702	4.583
10	36	85	4	90	3.644	6.13	3.644	6.129
11	36	85	6	50	3.579	4.72	3.912	4.720
12	36	85	8	70	3.572	4.419	3.572	4.419
13	36	90	4	70	3.555	5.051	3.555	5.051
14	36	90	6	90	1.258	3.34	1.260	3.340
15	36	90	8	50	2.121	4.368	2.706	4.392
16	36	95	4	90	2.346	4.584	2.346	4.607
17	36	95	6	50	2.53	4.325	3.070	4.325
18	36	95	8	70	2.746	4.688	2.746	4.688

4.1 ANOVA analysis

The ANOVA result unveils the influential factors of the input parameters (refer to Table 4). The regression statistics (R^2) exhibit values of 98.91% for CS and 98.52% for SR. Once the R^2 value approaches 100%, it indicates adequacy and fitness for estimated outcomes. Additionally, T_{on} emerges as the most significant parameter affecting CS (41.60% of PCR), followed by the interaction between T_{on} and WS (15.20% of PCR). Concerning SR, T_{on} is identified as the most significant parameter (22.32% of PCR), followed by the interaction between T_{on} and FR (17.12% of PCR). FR stands out as the least affected parameter for both response parameters.

Table 4. Analysis of Variance (Experimental)

Source	DF		Sum of Squares		Mean Squares		F		PCR	
	CS	SR	CS	SR	CS	SR	CS	SR	CS	SR
A	1	1	55.33	6.94	55.33	6.94	153.26	6.08	41.60	22.32
B	2	2	14.04	1.64	7.02	0.82	19.44	0.72	10.60	5.27
C	2	2	5.96	0.97	6.37	3.05	17.64	2.67	4.50	3.12
D	2	2	8.66	5.14	6.69	0.48	18.53	0.42	6.50	16.55
A*B	2	2	20.28	5.14	10.14	1.29	28.08	1.13	15.20	16.52
A*C	2	2	11.20	5.33	5.60	3.70	15.52	3.24	8.42	17.13
A*D	2	4	16.07	3.65	8.03	0.91	22.25	0.80	12.08	11.75
Residual Error	4	2	1.44	2.28	0.36	1.14			1.09	7.34
Total	17	17	132.99	31.09					100.00	100.00

4.2 Main Effect plots

Fig.5 illustrates the main effect plot for CS. Fig.5(A) shows a decrease in CS from 4.02 mm/min to 2.81 mm/min as T_{on} increases from level 1 to level 2. This increase in thermal energy with T_{on} may lead to more material melting. However, the constant flushing pressure causes the melted material to resolidify rapidly on the WEDMed surface, restricting CS and improving SR.

Moreover, Fig.5(B) indicates a decrease in CS from 3.79 mm/min to 3.18 mm/min as WS increases from level 1 to level 3. This reduction could be due to insufficient time for material melting as WS increases. Consequently, lower thermal energy results in less lumping of molten metal, reducing uneven craters in the machining zone and improving SR.

In Fig.5(C), the Cutting Speed (CS) increases from 3.23 mm/min to 3.57 mm/min as the Servo Sensitivity (FR) increases from level 1 to level 3. FR, responsible for minimizing error between GV and actual voltage, may enhance CS. Conversely, in their study, Mandal et al. [13] observed a link between reducing error and narrowing the Inter Electrode Gap (IEG) to lower GV. This observation suggests that decreasing error and narrowing the IEG may decrease thermal energy and surface roughness (SR).

Examining Fig.5(D), CS rises from 3.30 mm/min to 3.68 mm/min as GV increases from level 1 to level 2. This rise could be due to increased thermal energy with GV, enhancing CS. However, the deposition of molten material layers on the workpiece leads to an uneven surface, increasing SR.

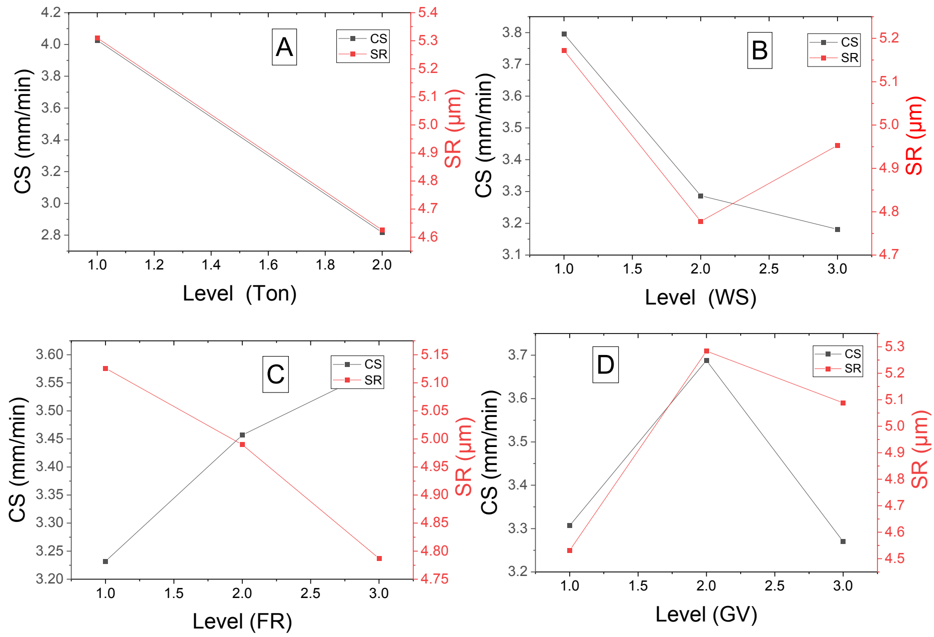

Fig. 5. Main effect plots (SR and CS)

4.3 ANN analysis

In this study, we employed ANN and nonlinear regression functions to train the experimental data. The ANN architecture comprised a 4-10-2 feed-forward neural network model utilizing the Levenberg-Marquardt learning algorithm. Fig.6 depicts the regression plot of the trained network. Additionally, Fig.7 illustrates the performance curve of the trained data. We utilized the trained response to formulate the equation based on the nonlinear regression model (multiplicative).

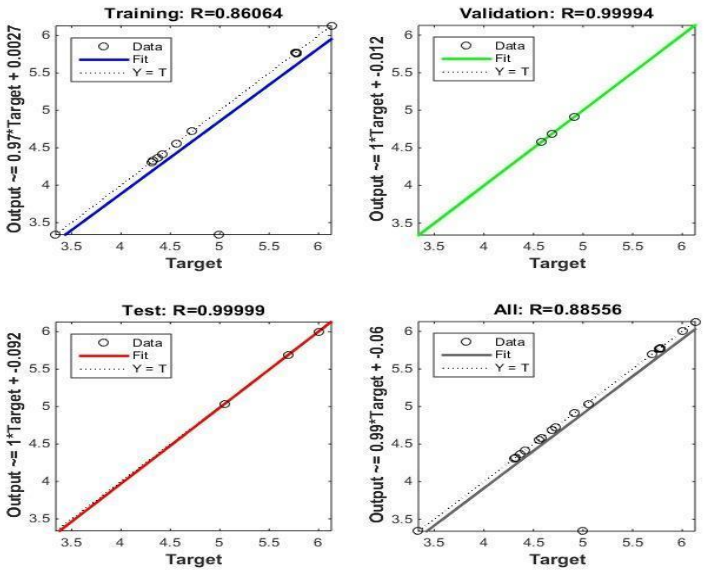

Fig.6. Regression-trained network plots

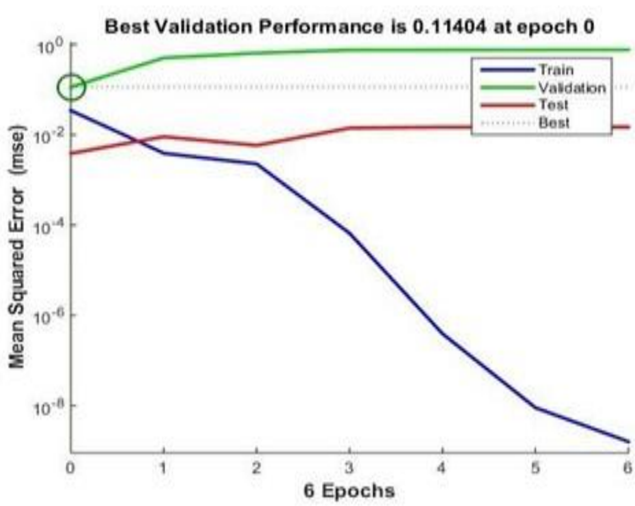

Fig.7. Performance curve of trend data

 https://doi.org/10.1051/e3sconf/202455201030

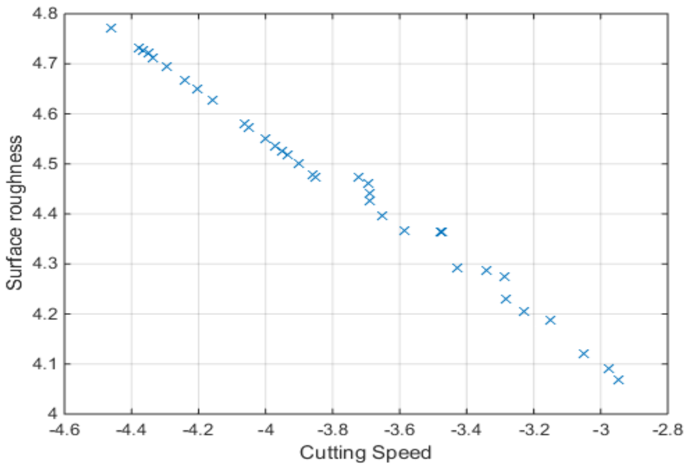

Fig.8. Pareto fronts for CS and SR using ANN-MOJAYA

4.4 Conformation test

Here, conformation tests were conducted on the ANN data using Eq.(i) to estimate the accuracy of the ANN. Table 5 illustrates that the Cutting Speed (CS) increases from 3 mm/min to 4.65 mm/min. Conversely, the Surface Roughness (SR) decreases from 4.99 µm to 4.32 µm. The conformational results indicate that ANN-MOJAYA yields superior outcomes for Inconel-690. The computational time for this hybrid technique was 4.65 seconds.

Table 5. Optimisation and Conformational test result

Rank	T_{ON}	WS	FR	GV	Optimisation result		Conformational test result		%error CS	%error SR	Computational time
					CS	SR	CS	SR			
1	36	95	8	50	2.95	4.07	3.00	4.39	1.697	7.883	3.65
2	36	90	8	50	2.98	4.09	3.20	4.48	7.411	9.539	4.82
3	32	85	8	50	4.38	4.73	4.61	4.93	5.406	4.227	5.68
4	32	85	8	50	4.36	4.73	4.65	4.98	6.499	5.367	3.42
5	32	85	8	50	4.46	4.77	4.62	4.85	3.592	1.630	5.74
6	36	95	8	50	3.05	4.12	3.25	4.32	6.554	4.853	3.90
7	32	85	8	50	4.35	4.72	4.49	4.96	3.244	5.044	5.04
8	32	85	8	50	4.34	4.71	4.51	4.97	3.996	5.496	4.85
9	32	85	8	50	4.33	4.71	4.48	4.91	3.388	4.244	3.76
10	32	85	8	50	4.30	4.69	4.43	4.99	3.114	6.392	4.13
11	32	85	8	50	4.24	4.67	4.42	4.87	4.290	4.263	3.42

5 Conclusions

The current study utilized Taguchi's L18 mixed-level design for experiments. We employed a Hybrid ANN-MOJAYA approach to optimize the machining parameters of WEDM for Inconel-690, with cutting speed (CS) and surface roughness (SR) examined as performance characteristics. The results are as follows:

1. We found Ton to have the most pronounced impact on CS and SR, while FR emerged as the least influential parameter.

2. Conformation test results revealed that parameters obtained from ANN-MOJAYA significantly improved overall machining performance, with maximum percentage errors of 7.41% for CS and 9.54% for SR.

3. The ANN-MOJAYA approach demonstrated minimal computational time and improved machining outcomes.

References

1. Smith, R., G. Lewi, and D. Yates, Development and application of nickel alloys in aerospace engineering. Aircraft engineering and aerospace technology, 2001. **73**(2): p. 138-147.
2. Rao, M.S., A.V.N. Babu, and N. Venkaiah, Modified flower pollination algorithm to optimize WEDM parameters while machining inconel-690 alloy. Materials Today: Proceedings, 2018. **5**(2): p. 7864-7872.
3. Manoj, I., et al. Investigation of machining parameters on corner accuracies for slant type taper triangle shaped profiles using WEDM on Hastelloy X. in IOP Conference Series: Materials Science and Engineering. 2019. IOP Publishing.
4. Selvakumar, G., et al., Enhancing die corner accuracy through trim cut in WEDM. The International Journal of Advanced Manufacturing Technology, 2016. **83**(5): p. 791-803.
5. Kumar, A., et al., Soft Computing Based Parametric Optimization of Cutting Rate, Surface Roughness, and Kerf Width in Wire Electric Discharge Machining of High Strength Ti-3Al-2.5 V. Experimental Techniques, 2023: p. 1-22.
6. Ehsan Asgar, M. and A.K. Singh Singholi. Parameter study and optimization of WEDM process: A Review. in Iop conference series: Materials science and engineering. 2018. IOP Publishing.
7. Ramakrishnan, R. and L. Karunamoorthy, Modeling and multi-response optimization of Inconel 718 on machining of CNC WEDM process. Journal of materials processing technology, 2008. **207**(1-3): p. 343-349.
8. Sibalija, T.V., et al., A soft computing-based study on WEDM optimization in processing Inconel 625. Neural Computing and Applications, 2021. **33**(18): p. 11985-12006.
9. Tarng, Y., S. Ma, and L. Chung, Determination of optimal cutting parameters in wire electrical discharge machining. International Journal of Machine Tools and Manufacture, 1995. **35**(12): p. 1693-1701.
10. Yusoff, Y., et al., Potential ANN prediction model for multiperformances WEDM on Inconel 718. Neural Computing and Applications, 2018. **30**: p. 2113-2127.
11. Shandilya, P., A.K. Rouniyar, and D. Saikiran, Multi-objective parametric optimization on machining of Inconel-825 using wire electrical discharge machining. Proceedings of the Institution of Mechanical Engineers, Part C: Journal of Mechanical Engineering Science, 2020. **234**(20): p. 4056-4068.
12. J Tapadar, R.T.P.C.S.K.T.S.S., Modeling of WEDM Parameters while Machining Mg-SiC Metal Matrix Composite. International Journal of Technology, 2017. **8**(5): p. 291-319.
13. Mandal, K., et al., Experimental investigation of process parameters in WEDM of Al 7075 alloy. Manufacturing Review, 2020. **7**: p. 30.